(6) Iskandarani, Z.; Miller, T. E. *Anal. Chem.* **1985**, *57*, 1591-1594.
(7) Issaq, H. J.; Mellini, D. W.; Beesley, T. E. *J. Liq. Chromatogr.* **1988**, *11*, 333-348.
(8) Issaq, H. J.; Gutierrez, J. *J. Liq. Chromatogr.* **1988**, *11*, 2851-2861.
(9) Risner, C. H.; Jezorek, J. R. *Anal. Chim. Acta* **1986**, *186*, 233-245.
(10) deBot, S. A.; Jezorek, J. R.; Hager, M. E. *J. Chromatogr.* **1989**, *465*, 249-262.
(11) Shahwan, G. J.; Jezorek, J. R. *J. Chromatogr.* **1983**, *256*, 39-48.
(12) Fulcher, C.; Crowell, M. A.; Bayliss, R.; Holland, K. B.; Jezorek, J. R. *Anal. Chim. Acta* **1981**, *129*, 29-47.
(13) Jezorek, J. R.; Faltynski, K. H.; Blackburn, L. G.; Henderson, P. J.; Medina, H. D. *Talanta* **1985**, *32*, 763-770.
(14) Jezorek, J. R.; Faltynski, K. H.; Finch, J. W. *J. Chem. Educ.* **1986**, *63*, 354-357.
(15) Faltynski, K. H.; Jezorek, J. R. *Chromatographia* **1986**, *22*, 5-12.
(16) Sugawara, K. F.; Weetall, H. H.; Schucker, G. D. *Anal. Chem.* **1974**, *46*, 489-492.
(17) Kuo, M.-S.; Mottola, H. A. *Anal. Chim. Acta* **1980**, *120*, 255-266.
(18) Jezorek, J. R.; Freiser, H. *Anal. Chem.* **1979**, *51*, 366-373.
(19) Marshall, M. A.; Mottola, H. A. *Anal. Chem.* **1983**, *55*, 2089-2093.
(20) Jezorek, J. R.; Fulcher, C.; Crowell, M. A.; Bayliss, R.; Greenwood, B.; Lyon, J. *Anal. Chim. Acta* **1981**, *131*, 223-231.
(21) Nondek, L.; Ponec, R. *J. Chromatogr.* **1984**, *294*, 175-183.
(22) Nondek, L.; Dienstbier, P.; Reriche, R. *HRC & CC, J. High Resolut. Chromatogr. Chromatogr. Commun.* **1988**, *11*, 217-218.
(23) Fritz, J. S.; Storey, J. N. *Anal. Chem.* **1974**, *46*, 825-829.
(24) Jezorek, J. R.; Freiser, H. *Anal. Chem.* **1979**, *51*, 373-376.

Helen W. Thompson
John R. Jezorek*

Department of Chemistry
University of North Carolina at Greensboro
Greensboro, North Carolina 27412-5001

RECEIVED for review June 7, 1990. Accepted October 12, 1990. This work was partially supported by the Research Council of the University of North Carolina at Greensboro.

TECHNICAL NOTES

Scanning Electrochemical Microscopy: Preparation of Submicrometer Electrodes

Chongmok Lee, Cary J. Miller, and Allen J. Bard*

Department of Chemistry, The University of Texas at Austin, Austin, Texas 78712

INTRODUCTION

In scanning electrochemical microscopy (SECM), a microvoltammetric tip electrode (e.g., microdisk geometry with a tip radius of the order of micrometers) is rastered in close proximity to the substrate to be imaged in a solution containing an electroactive species. In general, the steady-state tip current, i_T, is controlled by electrochemical reaction at the tip electrode and is a function of the solution composition, the tip–substrate distance, d, and the nature of the substrate itself. The measurement of i_T can thus provide information about the topography of the sample surface as well as its electrical and chemical properties (*1–4*). The lateral resolution of the scanning electrochemical microscope is governed by the size and shape of the voltammetric tip electrode and the ability to bring it into close proximity to the substrate surface ($d < 4r$, where the r is the radius of a tip) (*3*). To increase the lateral resolution of the SECM, it is therefore imperative to develop methodologies for fabricating tip electrodes having small (submicrometer) dimensions and an appropriate shape allowing their close approach to a substrate.

Because of the increasing interest in the properties and uses of ultramicroelectrodes, many procedures for their fabrication have been reported (*1*, *5–8*). Among the various types of microelectrodes (*5*), pulled-out Pt microdisk electrodes in glass (*6*) and Pt–Ir conical and hemispherical electrodes (*7*, *8*) could be used for SECM. Arrays of microdisk electrodes fabricated via electron beam lithography also have been reported (*9*, *10*). In this report, we describe two procedures for the construction of submicrometer microelectrodes particularly suited for use in SECM. In one, an electrochemically sharpened Pt wire is sealed in a glass capillary and the submicrometer tip is exposed via mechanical polishing, and in the other, electron beam lithography using a commercial scanning electron microscope is used to produce submicrometer features at the tip of a polymer-coated polished Pt wire. Moreover, this study demonstrates that submicrometer resolution in SECM characterization is possible with electrodes by these two techniques.

EXPERIMENTAL SECTION

Materials. Poly(methyl methacrylate) (950K molecular weight, 2% solution in chlorobenzene) and a mixture of methyl isobutyl ketone (MIBK) and isopropyl alcohol (IPA) (1:3 wt %) were obtained from KTI Chemicals (Sunnyvale, CA). Twenty grams of poly(methyl methacrylate) (very high molecular weight, Aldrich, Milwaukee, WI) was stirred in 100 mL of the MIBK–IPA mixture for 30 h. The remaining solid was filtered and dried in vacuo. All other chemicals were reagent grade and were used without further purification. Milli-Q reagent water (Millipore Corp., Bedford, WA) was used for the preparation of aqueous solutions. Pt wire (25-μm diameter) was obtained from Alfa (Ward Hill, MA). Silver-coated 2-μm- and 0.6-μm-diameter Pt wires were purchased from Goodfellow Ltd. (Malvern, PA). An interdigitated array (IDA) electrode consisting of 3-μm-wide Pt bands with 5-μm-wide SiO_2 spaces (for overall 8-μm periodicity) was generously provided by Dr. O. Niwa (NTT, Japan) (*11*).

Apparatus. Instrumental details and operational procedures for the SECM have been described previously (*4*). A JEOL JSM-35C scanning electron microscope (SEM) was used both for electron beam lithography and scanning electron micrographs. The progress of the electrode fabrication was monitored by using an optical microscope. Cyclic voltammetric experiments were performed with either a BAS 100A electrochemical analyzer or an SECM instrument. A microelectrode puller (Stoelting Co., Chicago, IL, catalog no. 51217) was used to draw capillary-end Pyrex tubing. Polymer thicknesses were measured by using a stylus profilometer (Alfa-step 200, Tencor Instruments, Mountain View, CA).

Microelectrode Preparation. *Method 1: Electron Beam Lithography.* Lengths of Pt wire (25-μm diameter) measuring 5 mm were bonded to a copper wire (1-mm diameter) by using Ag epoxy (H20S, Epotek) and subsequently sealed in vacuum epoxy (Torr-Seal, Varian). Figure 1 gives a schematic representation of the electrode fabrication procedure. The insulated wires were polished with 600-grit emery paper to expose the 25-μm cross section of the Pt wire. The Torr-Seal insulation was polished down to a ca. 200-μm diameter centered around the exposed Pt disk. Further polishing of the electrode using 1-μm-diameter alumina slurry resulted in the Pt wire protruding slightly from the epoxy insulation, as illustrated in Figure 1A. This was followed by a final polishing with 0.05-μm alumina. The electrodes were then dip-coated with a 5.5% solution of PMMA in chlorobenzene, dried in air, and heated in an oven at 50 °C for 1 h. The polymer-coated electrodes (PMMA thickness ~0.1–0.5 μm, Figure 1C) were mounted vertically onto an aluminum stub and placed

0003-2700/91/0363-0078$02.50/0

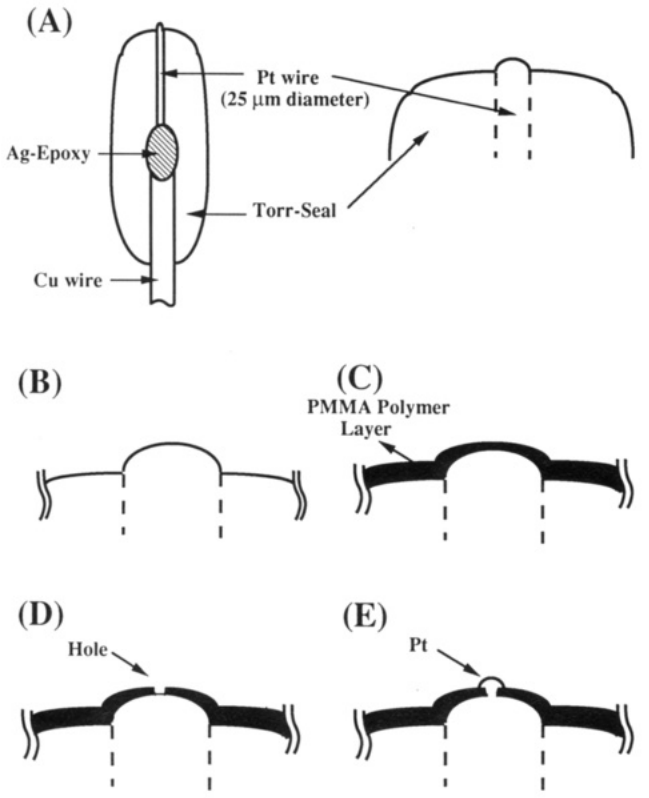

Figure 1. Schematic procedure for producing a microdisk electrode by electron beam lithography. (A) A cross section of the Pt electrode design and an enlarged view of the tip of the electrode after polishing. (B–E) Schematic representation of the Pt tip after polishing (B), coating with PMMA (C), developing the exposed area of the polymer to produce a cylindrical hole (D), and electroplating Pt into the exposed hole (E) (see text).

into the scanning electron microscope. After focusing and correcting for astigmatism, the electron beam was halted in the center of the Pt disk for 0.5 s at a beam current of 5–10 pA. The exposed polymer was removed by dropping 1 mL of a 1:3 mixture of MIBK and IPA on the surface, followed by a brief rinse with EtOH (Figure 1D). Pt was electroplated at −0.2 V versus Ag/AgCl, saturated KCl from a 1 mM H_2PtCl_6 solution in 0.1 M HCl. The electrolysis was halted once a predetermined amount of charge had passed (Figure 1E).

Method 2: Glass-Coated Electrode. A 1–2-cm-long Pt wire (25-μm diameter) was sharpened by electrochemical etching (*8*) in a solution of saturated $CaCl_2$ (60% v/v), H_2O (36%), and HCl (4%) at 2 V root-mean-square ac applied with a Variac autotransformer. A carbon rod served as the counter electrode in the two-electrode etching cell. A Pyrex capillary, tip diameter >100 μm, was drawn, using the microelectrode puller (heating setting 65, pulling setting 100), from a piece of Pyrex tubing (o.d. 2 mm and i.d. 1 mm). The tip of the capillary was sealed by heating for 1 s in a gas flame. The sharpened wire was transferred inside the glass capillary, and the open end of the tube was connected to a vacuum line and the capillary tip heated with four loops ($^1/_4$-in. i.d.) of nichrome wire (1.3-mm thick) at an ac voltage of 3.8 V ($T \approx 800$ °C). This resulted in the sealing of the Pt wire into the glass. Further manipulations involved in the fabrication of these electrodes are illustrated in Figure 2. Excess glass near the tip of the Pt wire (Figure 2A) was removed by heating the electrode in the resistive heater coil, which pulls the glass toward the Pt wire. Heating was halted just before the Pt tip was exposed (Figure 2B). The end of the electrode was then polished with 0.05-μm alumina paste until the tip of the sharpened Pt wire was exposed (Figure 2C). The diameter of the exposed Pt disk could be controlled from ca. 0.2 to 25 μm by controlling the extent of this final polishing. Further heating for 0.5–1 min caused the glass to pull away from the Pt wire so that the small exposed Pt disk protruded from the sealed glass (Figure 2D). Silver paint (E Kote No. 3030, Acme Products) was used for electrical connection to

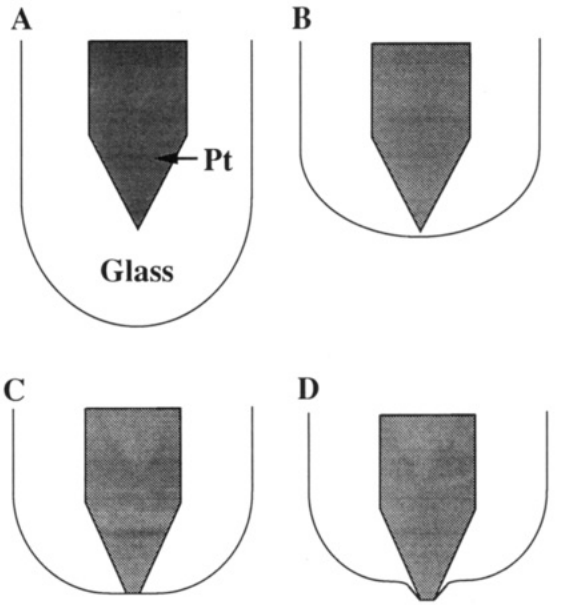

Figure 2. Schematic procedure for producing a sharp-end microdisk electrode sealed in glass (method 2, see text). (A) Sealing the etched Pt wire in glass under vacuum. (B) Allowing the excess glass at the electrode tip to flow by heating until the tip of the Pt wire is almost exposed. (C) Polishing to expose microdisk portion of wire. (D) Further heating, which results in the Pt disk protruding from the glass insulation.

the other end of the Pt wire. Other glass-coated electrodes were prepared by using 2- and 0.6-μm wire after etching the silver coating in 30% HNO_3 and sealing in glass following a previously reported procedure (*1*, *5*).

RESULTS AND DISCUSSION

In addition to fabricating electrodes with small exposed surface areas, it is crucial that SECM electrode tips have the appropriate geometry. Because the active electrode area must approach the surface to be imaged very closely (within approximately the diameter of the electrode surface), the surrounding insulation cannot extend beyond the metal electrode. Clearly the exposed Pt must also be at the lowest point of the electrode structure. These considerations, important in SECM, are of less significance in the fabrication of ultramicroelectrodes for conventional voltammetric studies. For this reason, it is beneficial to minimize the diameter of the insulation and to allow the active electrode area to protrude slightly from the plane of the insulation. Moreover, it is desirable to be able to control the diameter of the electrode, producing a given sized electrode at will rather than by chance. Both of the electrode fabrication schemes described here allow this degree of control of the electrode size and geometry.

Electron Beam Lithography. In electron beam lithography, a focused electron beam is guided across a sensitive polymer-coated substrate. The polymer is subsequently developed in an appropriate solvent to reveal the electron beam's path. High molecular weight PMMA has been used extensively as an electron beam resist. The exposure to the electron beam causes cleavages in the polymer chains, lowering the molecular weight of the polymer and increasing its solubility in certain organic solvents (*12*). The resolution at which features can be written on surfaces depends primarily on the size of the electron beam. In a typical SEM, one can easily focus the electron beam to a diameter less than 1000 Å, allowing one to produce small circular electrodes with submicrometer dimensions.

Some attention must be given to the construction of the polymer-coated electrodes prior to their exposure to the electron beam. The Torr-Seal epoxy insulation, which is approximately 2 mm in diameter, is polished away from the

Table I. Correlation between the Interference Color and the Thickness of the PMMA Layer

interference color[a]	polymer thickness,[b] μm
(faint yellow)	<0.1
gray–blue	0.11
yellow	0.20
violet–red	0.25
blue	0.29
yellow	0.38
red–violet	0.46
green	0.53
red	0.63
blue–green	0.70
orange	0.77
green	>0.8
red	
green	

[a] Color viewed at normal incidence. [b] Thickness measured in the middle of the interference band.

25-μm-diameter Pt disk at a ca. 45° angle taper leaving approximately a 100–200-μm-diameter top face surrounding the electrode. Because the epoxy is removed more quickly than the Pt electrode, further polishing of the top face of the electrode results in the Torr-Seal insulation curving away from the Pt electrode and a gentle rounding of the Pt disk into a flattened hemisphere. This geometry allows the electrode surface to come in close proximity to a substrate even if there is some misalignment of the SECM tip electrode relative to the surface of the substrate. The final polishing with 0.05-μm alumina is continued until no imperfections are visible under 100× magnification in an optical microscope. Imperfections such as polishing scratches and pits cause discontinuities in the PMMA polymer coating.

The dip-coating procedure was found to produce PMMA layers of widely varying thickness depending on the exact conditions of the deposition, especially the radius of curvature of the Pt disk and the speed at which one withdraws the electrode from the 5.5% PMMA solution. The thickness of the polymer layer on the Pt disk was monitored by noting the interference color on the electrode after dip coating in the 5.5% PMMA solution. Table I gives the polymer thickness as a function of the interference color. These data were obtained by dip coating a Si wafer, allowing it to dry in a vertical orientation, and then removing part of the polymer layer by a brief exposure to sulfochromic acid (saturated $K_2Cr_2O_7$ in H_2SO_4). The interference colors were noted at a normal angle and the polymer thicknesses measured with a stylus profilometer. There were usually several different interference colors visible on the polymer-coated Pt electrodes because of different layer thicknesses across the film (see Figure 1C). This procedure allows one to determine uniquely the polymer thickness at any location. Polymer thicknesses within the range 0.1–0.5 μm gave the best results. Thinner polymer layers did not block the unexposed electrode surface adequately, and substantially thicker layers were impossible to image in the SEM due to the poor conductivity of the polymer-coated electrode, which results in charging of the polymer surface and severe distortion of the SEM image.

The exposure of a single submicrometer spot on the PMMA-coated Pt disk presents several challenges. Because the height of each electrode in the aluminum SEM stub varies, the electron beam must be focused for each electrode. The difficulty here is that, during the focusing of the electron beam on the tip of the polymer-coated electrode, one must avoid inadvertently exposing areas of the Pt disk by using a very low beam current (5–15 pA) and a low magnification (which rasters the electron beam rapidly over a large area so that any individual spot on the polymer does not receive sufficient electron exposure to be dissolved under the developing conditions). Once the Pt disk is located on the tip of the electrode, the beam is focused on an adjacent area of the Torr-Seal epoxy. At a magnification of 500–1000X and a beam current of 5–10 pA, the Pt disk is positioned in the center of the microscope field of view and the beam is halted at the center for a short period of time, resulting in the exposure of a small dot at the center of the Pt disk. At a beam current of 10 pA and a magnification of 1000X, the electrode can be viewed for several minutes without any appreciable exposure of the polymer film.

The size of the final electrode can be controlled several ways. One can purposefully defocus the electron beam to create circular electrodes of an arbitrary size. To implement this strategy successfully, one must calibrate the fine focus control on the SEM and increase the exposure time or beam current according to the beam size. Alternatively, one can bring the electron beam into a fine focus (below 0.1-μm diameter) and increase the exposure time. In this case, secondary electrons that are scattered from the Pt surface expose the polymer radially from the primary electron beam. Increasing the exposure time from 0.5 to 10 s (at 10-pA beam current) results in the diameter of the exposed area increasing from ca. 0.5 to 6 μm. Finally, one can create a small hole in the PMMA layer and electroplate Pt into the hole until an electrode of a desired size is deposited, as is shown in Figure 1E. In this way, the electrode surface can be made to protrude from the PMMA insulation, allowing its close approach to a substrate surface.

Glass-Coated Electrode. The fabrication of these electrodes relies on the tendency of melted glass to flow. At several stages in the electrode fabrication scheme, the glass-coated wire is heated, allowing the glass to thicken and pull away from the Pt tip. At the sealing stage, the application of a vacuum is necessary to avoid bubbles inside the glass. These small bubbles distort the flow of molten glass and in many cases ruin the electrode geometry. During the sealing step and the thinning of the glass insulation (shown in Figure 2A,B), there is the possibility that the tapered end of the Pt wire will bend as it is pulled with the molten glass. To avoid this bending, the tapered end of the etched wire should be less than ca. 50 μm in length. This short taper length can be obtained by slowly withdrawing the Pt wire from the etching cell at a higher ac voltage (e.g., a rate of 0.5 mm/min and 13 V) during the electrochemical etching of the wire. When the Pt end of a tip is exposed during the polishing step, it can be seen with an optical microscope by varying the nature of the illumination. When illumination is through the objective lens, the exposed Pt disk appears as a bright dot, while illumination from beneath the sample causes the Pt disk to appear as a dark spot. The ultimate Pt disk size is governed by the sharpness of the etched tip and the ability to stop the mechanical polishing at the point when the tip of the Pt wire is just exposed. These two factors made the fabrication of very small tip diameters challenging. Only 10% of the electrodes had a diameter of less than 0.3 μm. By omitting the polishing step (Figure 2C), a glass-coated scanning tunneling microscope (STM) tip could be obtained (conical shape; similar to those in ref 7). In this case, heating at a higher setting and for a longer time was required to uncover the end of a tip. For these STM electrodes, the current of the exposed area was consistent with a 0.5–5-μm-diameter microdisk electrode.

Electrode Characterization. The electrodes were first characterized by cyclic voltammetry. Figure 3A shows the voltammetric signal for a 0.1 M ferrocyanide solution using an exposed PMMA-coated electrode after developing. Before the exposed polymer is dissolved, no voltammetric wave can

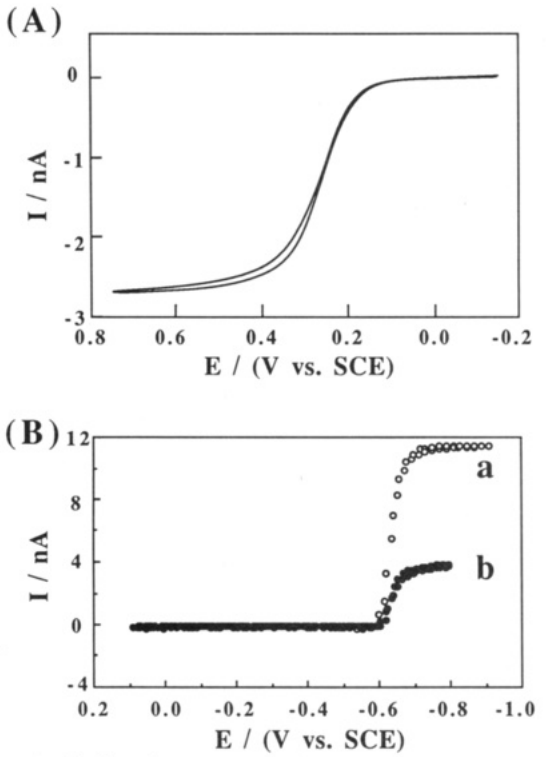

Figure 3. Cyclic voltammograms of microelectrodes. (A) Method 1 electrode: solution, 0.1 M $K_4Fe(CN)_6$ and 1 M KCl; scan rate (v) of 0.1 V/s. (B) Solution, 0.2 M $MVCl_2$ and 2 M KCl: (a) glass-coated electrode using 0.6-μm-diameter commercial wire; v = 1 V/s; (b) small method 2 electrode; v = 0.1 V/s.

be detected, demonstrating that the PMMA layer is able to block completely the 25-μm Pt disk. After developing, a sigmoidal voltammetric wave characteristic of a small microelectrode is seen. The radius of the microelectrode can be estimated by the diffusion-limited plateau current, i, by using the relation (5)

$$i = 4nFDCr \quad (1)$$

where n is the number of electrons transferred per molecule, F is Faraday's constant, D is the diffusion coefficient of the redox species, C is the bulk concentration of the redox species, and r is the radius of the microdisk electrode. The calculated diameter of the electrode using eq 1 (0.25 μm) will be somewhat smaller than the true one, because the electrode is recessed by the thickness of the polymer layer (ca. 0.25 μm). Figure 3B shows cyclic voltammograms (CV) obtained in a 0.2 M solution of methyl viologen (MV) dichloride, 2 M KCl using a microelectrode fabricated by using method 2 and one fabricated by using a 0.6 μm wire. By comparison with the CV of the 0.6-μm-diameter electrode, the size of the microelectrode produced by method 2 was determined to be approximately 0.2 μm in diameter.

The geometry and size of these microelectrodes was also investigated by scanning electron microscopy. For parts A, C, and D of Figure 4, 300 Å of Au was sputtered onto the electrodes to reduce the surface charging. Parts A and B of Figure 4 show the exposed Pt tip of two separate electrodes made by using the electron beam lithographic technique (method 1). The Au sputtering, which was used to image the cylindrical holes produced in the PMMA layer, was observed to enlarge the holes and produce irregular edges by comparison with SECM images of holes seen initially without Au coating. The electrode shown in Figure 4B was produced by electrodepositing Pt into the lithographically generated hole. An electric charge of 2×10^{-8} C was passed during the electrolysis corresponding to approximately 0.5-μm thickness in the ca. 1-μm hole. Because the polymer layer was only 0.25-μm thick in this case, the Pt electrode should extend beyond the polymer insulation. Parts C and D of Figure 4 show a top view and a side view of a glass-coated electrode produced by the mechanical polishing method (method 2). The cross section

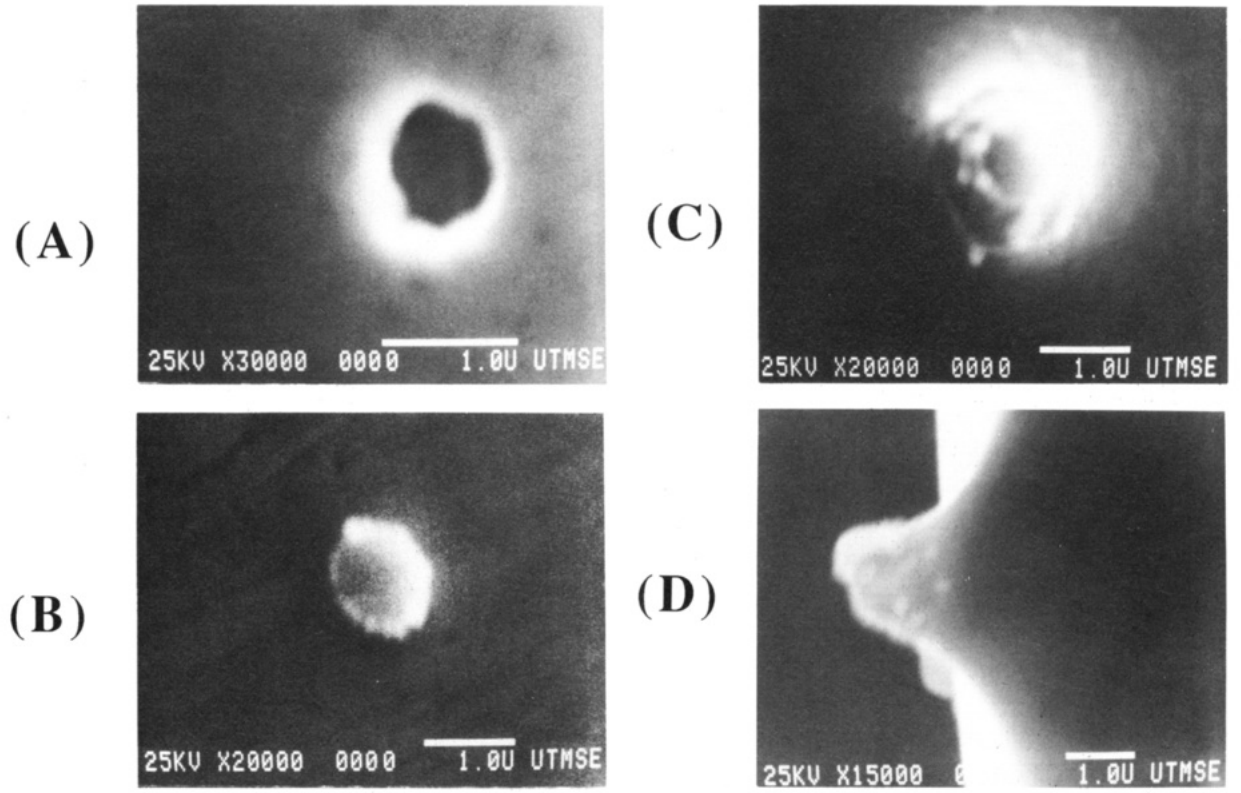

Figure 4. Scanning electron micrographs of the microelectrodes. (A) An electrode beam lithographically produced hole in the PMMA polymer layer. (B) An electron beam lithographically produced electrode after the electrodeposition of Pt (see text). (C) A top view and (D) side view of glass-coated Pt electrode.

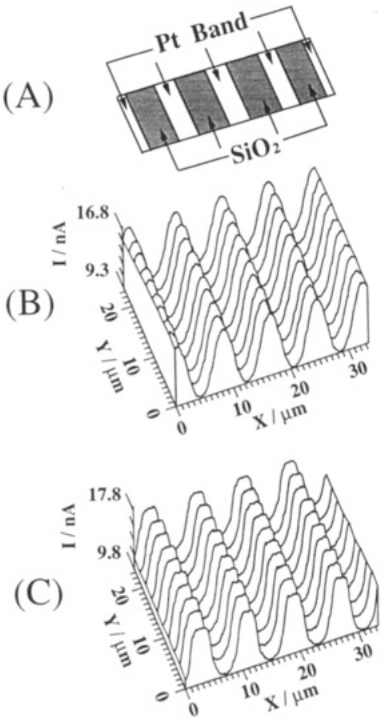

Figure 5. (A) Schematic diagram of IDA. Scans of an IDA, potential of tip electrode, E_T, of −0.78 V vs SCE: (B) tip, 2-μm-diameter Pt microdisk electrode; solution, 40 mM $MVCl_2$ and 2 M KCl; $i_{T,\infty}$ − 11.4 nA; (C) tip, 0.6-μm-diameter Pt microdisk electrode; solution, 0.2 M $MVCl_2$ and 2 M KCl; $i_{T,\infty}$ = 13.6 nA.

of the tip of the glass-coated Pt tip is in good agreement with the size measured for this electrode by cyclic voltammetry using eq 1 (0.6-μm diameter).

Scanning Electrochemical Microscopy. SECM was used in obtaining information about these electrodes (e.g., relative size of electrode, stability of current, position of exposed disk). To demonstrate the effect of tip size on SECM resolution, SECM scans of an IDA with 0.6-μm- and 2-μm-diameter electrodes prepared from commercial, unetched, Wollaston Pt wire are shown (Figure 5). The aqueous solution in which the IDA was immersed contained 40 mM or 0.2 M $MVCl_2$ and 2 M KCl. The scans were made across the IDA bands, with the tip held at −0.78 V where the reduction of MV^{2+} to MV^+ occurs. The SECM response depends upon surface conductivity. A positive feedback is observed ($i_T > i_{T,\infty}$, where $i_{T,\infty}$ is the tip current when the tip is held far from the substrate) when the tip is over the Pt band because of regeneration of MV^{2+} at the conducting band. When the tip passes over the SiO_2 area, where no regeneration of the MV^{2+} species can occur, only the shielding of the hemispherical diffusion by the insulating sheath surrounding the Pt can be seen, resulting in a negative feedback ($i_T < i_{T,\infty}$). The average periodicity of Pt bands in the IDA is in good agreement with the specified spacings (3-μm Pt band, 0.1-μm thick, and 5-μm SiO_2 gap, with an overall 8-μm periodicity). Since the tip diameter was similar to the width of the Pt bands, the change of the current as the tip electrode moved across the Pt bands showed a sinusoidal rather than a step shape (Figure 5B). With the smaller electrode (Figure 5C), the SECM image showed the flat portion of Pt bands and a trapezoidal shape. Higher resolution scans were obtained with electrodes prepared by the methods described here. Figure 6 shows an SECM scan of the same IDA with a small (method 2) electrode (~0.2-μm diameter). Note that the current change pattern shows a clear steplike shape. However, with this electrode, negative feedback is not shown when the electrode is over the insulating (SiO_2) portion of the IDA (i.e., i_T is not decreased compared to $i_{T,\infty}$). This is consistent with the very thin glass

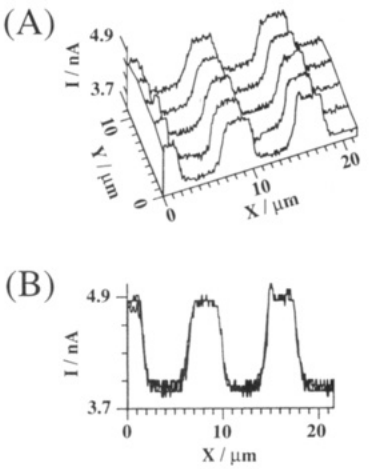

Figure 6. Scan of an IDA: tip, small glass-coated electrode (ca. 0.2-μm diameter, method 2); $i_{T,\infty}$ = 3.7 nA; E_T = −0.76 V vs SCE; solution, same as in Figure 4B. (A) Three-dimensional view; (B) side view.

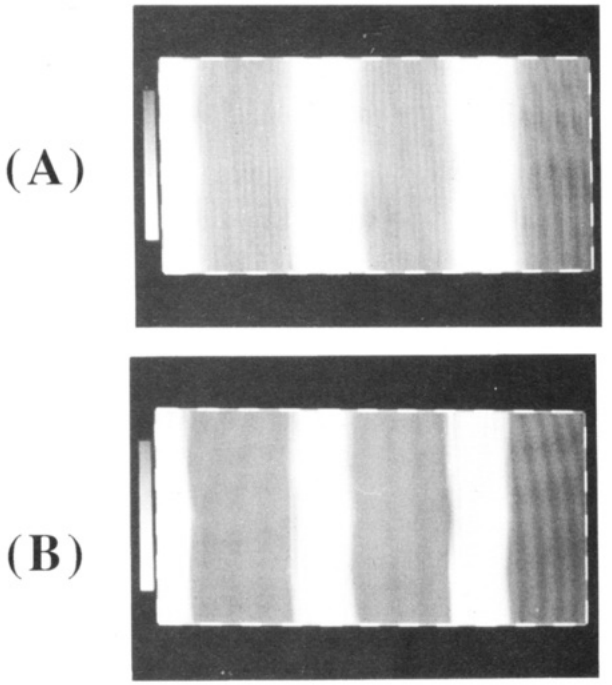

Figure 7. Gray-scaled images of Figure 6. The white lines around the edge denote a 1-μm distance, and the scale at the left shows the gray-scale variation: light color, large cathodic current; dark color, small cathodic current, (A) from minimum to maximum current of Figure 6; (B) from average to maximum current of Figure 6.

insulator sheath around the exposed Pt tip, which does not hinder appreciably diffusion of MV^{2+} to the Pt when the tip is close to the substrate (*4*). This implies that these (method 2) electrodes will not be useful in imaging insulating substrates. Figure 7 is a gray-scale presentation of the data of Figure 6, where the variation of i_T was converted to a color intensity. Light shades represent maximum i_T (Pt bands) and dark shades minimum i_T. Figure 7 clearly shows submicrometer resolution in the SECM images. Better resolution than that in Figure 5C was obtained by using a (method 1) electrode (~0.5-μm diameter) for the SECM scan, especially over the insulating region (Figure 8).

CONCLUSIONS

Two methodologies for the construction of submicrometer SECM tips are reported. Both methods described here are easily implemented by using equipment common to most laboratories. In addition to their use in the SECM, electrodes

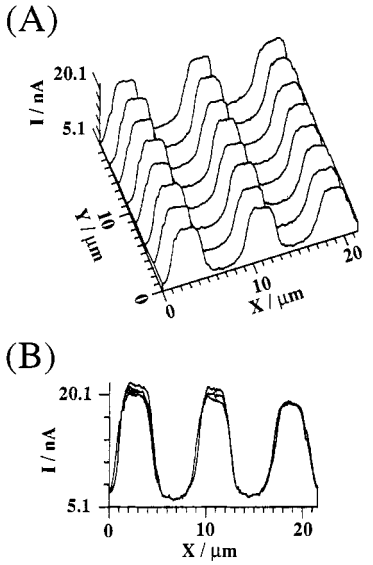

Figure 8. Scan of an IDA: tip, a method 1 electrode (~0.5-μm diameter, a Pt hole in a <0.3-μm-thick PMMA layer, see Figure 1D); $i_{T,\infty}$ = 12.5 nA; E_T = -0.77 V vs SCE; solution, same as in Figure 4B. (A) Three-dimensional view; (B) side view.

of these types could be equally useful in voltammetric studies and in STM experiments performed in situ in electrolyte solution. Their controllable sizes and predictable geometries are especially important in the SECM experiment. The implementation of mathmatical (e.g., deconvolution) schemes should improve the resolution of the SECM but would require electrodes with well-characterized shapes. While it is unlikely that the resolution of SECM will ever approach that of STM (atomic resolution), improvements to bring SECM to the level of several tens of nanometers, by reduction in tip size and by employing deconvolution or tomographic-type techniques, should be possible.

ACKNOWLEDGMENT

We acknowledge the assistance of I. Trachtenberg, M. Schmerling, and Daniel Mandler and the donation of the IDA by O. Niwa. This is paper number 6 in the SECM series.

LITERATURE CITED

(1) Bard, A. J.; Fan, F.-R. F.; Kwak, J. Lev. O. *Anal. Chem.* **1989**, *61*, 132.
(2) Bard, A. J.; Denuault, G.; Lee, C.; Mandler, D.; Wipf, D, O. *Acc. Chem. Res.*, in press.
(3) Kwak, J.; Bard, A. J. *Anal. Chem.* **1989**, *61*, 1221.
(4) Kwak, J.; Bard, A. J. *Anal. Chem.* **1989**, *61*, 1794.
(5) Wightman, R. M.; Wipf, D. O. In *Electroanalytical Chemistry*; Bard, A. J., Ed.; Marcel Dekker: New York, 1989; Vol. 15, pp 267-353 and references therein.
(6) Pendley, B. D.; Abruña, H. D. *Anal. Chem.* **1990**, *62*, 782.
(7) Penner, R. M.; Heben, M. J.; Lewis, N. S. *Anal. Chem.* **1989**, *61*, 1630.
(8) Gewirth, A. A.; Craston, D. H.; Bard, A. J. *J. Electroanal. Chem. Interfacial Electrochem.* **1989**, *261*, 477.
(9) Hepel, T.; Osteryoung, J. *J. Electrochem. Soc.* **1986**, *133*, 752.
(10) Hepel, T.; Osteryoung, J. *J. Electrochem. Soc.* **1986**, *133*, 7577.
(11) Aoki, K.; Morita, M.; Niwa, O.; Tabei, H. *J. Electroanal. Chem. Interfacial Electrochem.* **1988**, *256*, 269.
(12) Greeneich, J. S. In *Electron Beam Technology in Microelectronic Fabrication*; Brewer, G. R., Ed.; Academic Press: New York, 1980; Chapter 2.

RECEIVED for review July 9, 1990. Accepted September 28, 1990. The support of this research by NSF (CHE 8901450) and the Texas Advanced Research Program is gratefully acknowledged.

Vibrating Mirror Surface Plasmon Resonance Immunosensor

Rob P. H. Kooyman,* Aufried T. M. Lenferink, Rob G. Eenink, and Jan Greve

Department of Applied Physics, Twente University, P.O. Box 217, 7500 AE Enschede, The Netherlands

INTRODUCTION

In the past few years, much scientific and industrial effort has been put in the development of immunosensors (*1*). In these chemical sensors, antibodies are used as selector molecules to quantitatively determine the presence of a specified analyte, typically a protein. One class of optical immunosensors consists of devices where the optical evanescent field is exploited to probe changes at the interface between solution and antibody-covered substrate as a result of the binding between antibody and analyte.

The utilization of surface plasmon resonance (SPR) has been shown to be a promising method to be implemented in the development of these types of immunosensors (*2-4*). Generally, the angular-dependent reflectivity of light falling on a silver-coated prism onto which antibodies are immobilized provides information on the refractive index profile in the immediate vicinity (~100 nm) of the interface, which can be interpreted in terms of the coverage of antibodies (*2*). As it is beyond the scope of the present paper, we will not discuss the theory of SPR (for a review, see ref 5); for our purposes, it suffices to mention that in the present context the main experimental parameter of a SPR experiment is the rate of change of angular position of the reflectivity minimum. We will focus on the experimental determination of this parameter.

From previous experiments, it is known (*2*) that in order to measure protein concentrations of the order of 1 nM one has to obtain an angular resolution of the order of 10^{-2} deg, given a plasmon resonance curve with a width of 2 deg. Several experimental approaches have been applied, such as monitoring the reflectivity in the region of maximum slope (*3*) and the use of photodiode arrays (*6*). A particularly elegant method was recently published, where use was made of an etched grating (*4*). This device, however, presently suffers from lack of sensitivity.

In the following, we will describe another method with properties that make it well suited for its use in the construction of SPR-based immunoassays.

EXPERIMENTAL SECTION

Figure 1a shows the optical arrangement. The sensor element consists of a glass microscope slide (Chance), coated with a silver layer of ~50-nm thickness, and optionally a polystyrene overlayer of about 20 nm (*2*).

Before the silver-coating procedure, the slides were cleaned by soaking in a detergent solution at 90 °C in an ultrasonic bath for ~30 min and subsequent rinsing in deionized water.

* Author to whom correspondence should be addressed.

0003-2700/91/0363-0083$02.50/0